

# The $\phi^4$ Model, Chaos, Thermodynamics, and the 2018 SNOOK Prizes in Computational Statistical Mechanics

Wm.G. Hoover, C.G. Hoover

*Ruby Valley Research Institute  
Highway Contract 60, Box 601, Ruby Valley, Nevada 89833, USA  
E-mail: hooverwilliam@yahoo.com*

Received: 09 June 2018; accepted: 11 June 2018; published online: 30 June 2018

**Abstract:** The one-dimensional  $\phi^4$  Model generalizes a harmonic chain with nearest-neighbor Hooke's-Law interactions by adding quartic potentials tethering each particle to its lattice site. In their studies of this model Kenichiro Aoki and Dimitri Kusnezov emphasized its most interesting feature: because the quartic tethers act to scatter long-wavelength phonons,  $\phi^4$  chains exhibit Fourier heat conduction. In his recent Snook-Prize work Aoki also showed that the model can exhibit chaos on the three-dimensional energy surface describing a two-body two-spring chain. That surface can include *at least two* distinct chaotic seas. Aoki pointed out that the model typically exhibits *different* kinetic temperatures for the two bodies. Evidently few-body  $\phi^4$  problems merit more investigation. Accordingly, the 2018 Prizes honoring Ian Snook (1945-2013) will be awarded to the author(s) of the most interesting work analyzing and discussing few-body  $\phi^4$  models from the standpoints of dynamical systems theory and macroscopic thermodynamics, taking into account the model's ability to maintain a steady-state kinetic temperature gradient as well as at least two coexisting chaotic seas in the presence of deterministic chaos.

**Key words:**  $\phi^4$  model, chaos, Lyapunov exponents, algorithms

---

## I. THE SIMPLEST $\phi^4$ CHAIN AND THE 2018 SNOOK PRIZES

The 2017 Snook Prize has already shed considerable light on small-system implementations of Kenichiro Aoki and Dimitri Kusnezov's  $\phi^4$  Model [1]. Besides providing transparent time-reversible examples of nonequilibrium heat flows the model illustrates several varieties of broken symmetries in both space and time, as discussed elsewhere in this issue of Computational Methods in Science and Technology [2, 3]. Fig. 1 shows equally-spaced contours of the kinetic and potential energies of the model.

For simplicity, in this work we take initial conditions where the energy is entirely kinetic,  $q_1 = q_2 = 0$ ;  $p_1^2 + p_2^2 = 12$ . The examples here correspond to the same energy states studied by Aoki and illustrated in Figs. 6 and 7 of his prize-winning contribution for last year's Snook Prizes [2, 3].

In that same competition Timo Hofmann and Jochen Merker discovered two *coexisting* chaotic seas in a fourteen-term polynomial generalization of the Hénon-Heiles model's cubic Hamiltonian [4]. In our follow-up exploration of the two-body  $\phi^4$  model we have found two coexisting chaotic seas. Specimens of both are shown in Figs. 2 and 3. Evidently the present simplest of chaotic Hamiltonians, with only seven polynomial energy contributions, is enough to support the coexistence of the seas.

## II. CHAOS IN THE TWO-MASS $\phi^4$ CHAINS

Relatively long calculations with  $10^{11}$  timesteps showed that both of the problems solved in Figs. 2 and 3 are chaotic. We used the same reference trajectory + rescaled-satellite trajectory algorithm discovered independently by groups in

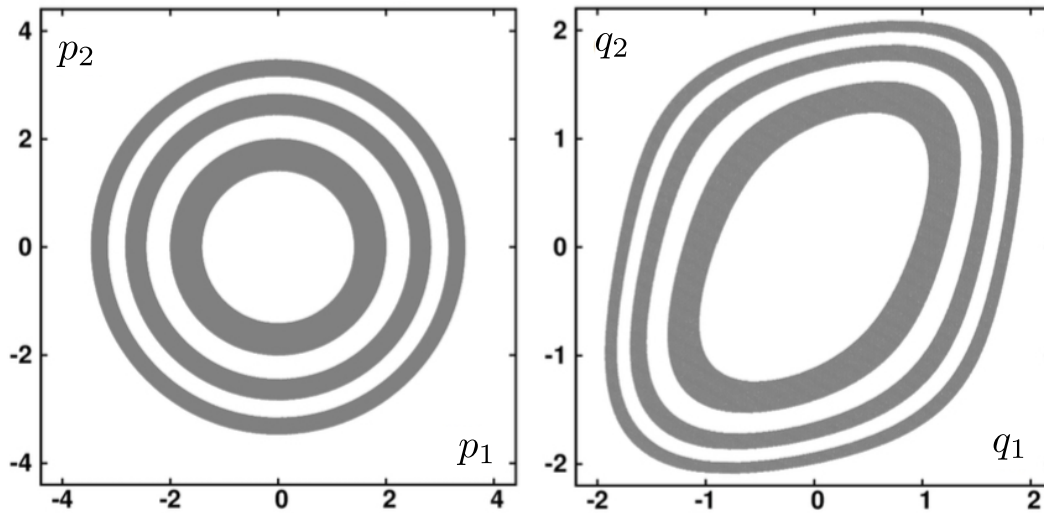
Phase-Space States with  $E < 6$ 

Fig. 1. When the two-body  $\phi^4$  model has an energy of 6, the momenta are confined to the region  $p_1^2 + p_2^2 < 12$  shown at the left. The displacement coordinates of the particles,  $q_1$  and  $q_2$ , are confined to the region shown to the right. The contours shown here correspond to the energies 1 through 6.  $E = [p_1^2 + p_2^2 + q_1^2 + (q_1 - q_2)^2]/2 + (q_1^4 + q_2^4)/4 < 6$ . Most of the three-dimensional microcanonical energy shell between  $E = 6$  and  $E = 6 + dE$  corresponds to stable tori

Italy and Japan [5, 6]. The small sea in Fig. 3 corresponds to a Lyapunov exponent of 0.003.

exponent description of the divergence of two nearby trajectories is defined by the rate equations  $\{\dot{\delta} = \lambda_1 \delta\}$ , where the separation  $\delta$  is measured in phase space:

$$\delta \equiv \sqrt{\delta_{q_1}^2 + \delta_{q_2}^2 + \delta_{p_1}^2 + \delta_{p_2}^2}.$$

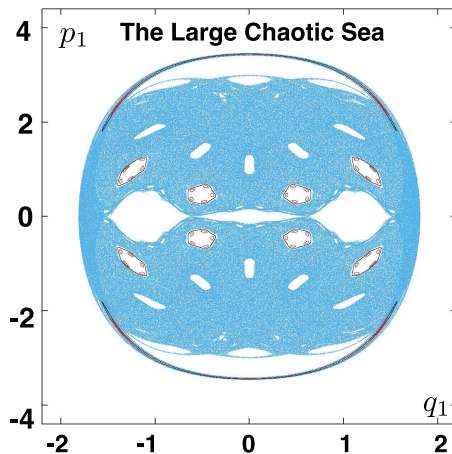


Fig. 2. A projected section of the “Large” sea generated with initial conditions  $(q_1, q_2) = (0, 0)$  and  $(p_1, p_2) = (\sqrt{12}, 0)$  is shown in blue. Most of the phase space at this energy corresponds to tori. The two toroidal examples shown here correspond to initial momenta of  $(\sqrt{(11.9, 0.1)})$  and  $(\sqrt{(11.8, 0.2)})$ , with each point on the closed curves plotted when the trajectory passes through the  $q_2 = 0$  hyperplane

The large sea of Fig. 2 is much less stable, with a time-averaged exponent  $\lambda_1 = 0.05$ . We wish to emphasize that these two values correspond to exactly the same energy, 6, and only differ in the initial values of  $p_1$  and  $p_2$ . The Lyapunov-

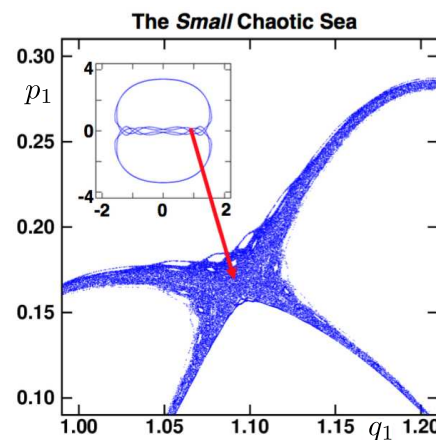


Fig. 3. Here the initial condition is  $(q_1, q_2) = (0, 0)$  and  $(p_1, p_2) = (\sqrt{(11.4, 0.6)})$  and the projection onto the  $(q_1, p_1)$  plane is done whenever  $q_2 = 0$ . The full projection is shown in the upper left inset, where  $|q_1| < 2$ . An enlargement shows that the apparent crossing lines in the inset actually correspond to “fat fractal” regions with a nonvanishing Lyapunov exponent,  $\lambda_1 = 0.003_0$ , where the simulation was extended for  $10^{11}$  timesteps in order to get a reliable value of the exponent

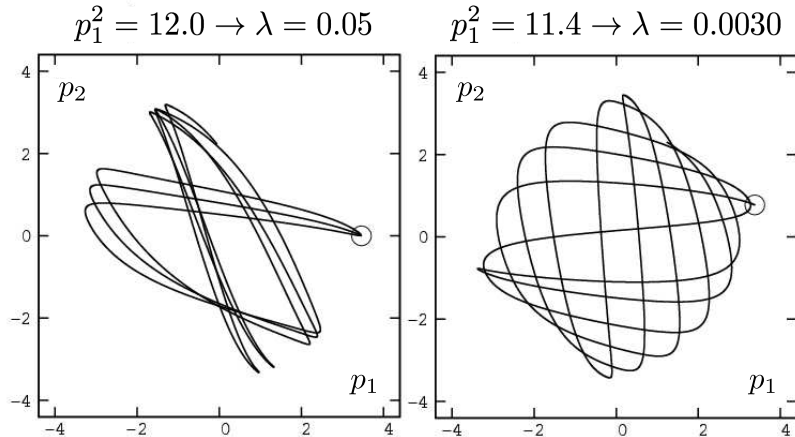


Fig. 4. Starting with two circled initial conditions ( $p_1^2 = 12$ ;  $p_2^2 = 0$ ) and ( $p_1^2 = 11.4$ ;  $p_2^2 = 0.6$ ) we show the  $(p_1, p_2)$  trajectory projections in momentum space up to a time of 20. These two trajectories are both chaotic, but with very different Lyapunov exponents

The rescaling algorithm brings the satellite trajectory to the same distance,  $\delta \rightarrow 0.00001$ , after each timestep. We use fourth-order or fifth-order Runge-Kutta integrators with  $dt = 0.001$  throughout.

Fig. 4 shows the momenta for a time interval  $0 < \text{time} < 20$  for the large and small seas. It is a little paradoxical that the less stable large-sea trajectory (at the left, with  $\lambda_1 = 0.05$ ) apparently explores *less* of the  $(p_1, p_2)$  region than does the more-stable  $\lambda_1 = 0.003_0$  small-sea trajectory.

The three-dimensional energy surface in four-dimensional phase space,  $\{q_1, p_1, q_2, p_2\}$  is difficult to visualize. Lacking a clever coordinate transformation we can only project or cut. Investigation of two-dimensional projections on the six two-dimensional planes provided by the four state variables shows that much of the surface is composed of tori. For initial conditions with all or nearly all of the kinetic energy given to Particle 1 at least two chaotic seas occur. The sections in Fig. 5 show the chains of islands typical of Hamiltonian chaos as well as the structures corresponding to simple elliptic doughnuts. It appears that the chaotic regions correspond to three-dimensional “fat fractals” [7]. The sections provide plenty of room for further exploration.

### III. THERMODYNAMICS AND THE IDEAL-GAS THERMOMETER

It is interesting to see that the time-averaged kinetic temperatures of the two particles,  $T_i = \langle p_i^2 \rangle$ , are quite different in both the large unstable and the small more stable chaotic seas. A permanent temperature difference in a stationary equilibrium system suggests thought-experiments violating the Second Law of Thermodynamics. Evidently ideal-gas thermometers, though validated by kinetic theory [8] cannot be entirely consistent with equilibrium thermodynamics. This subject is complicated by the fact that nonequilibrium frac-

tal distributions (typically found for time-reversible steady states) [9] correspond to a divergence of the Gibbs entropy  $S$ , making the usual equilibrium definition of temperature,  $(\partial E / \partial S)_V$ , useless.

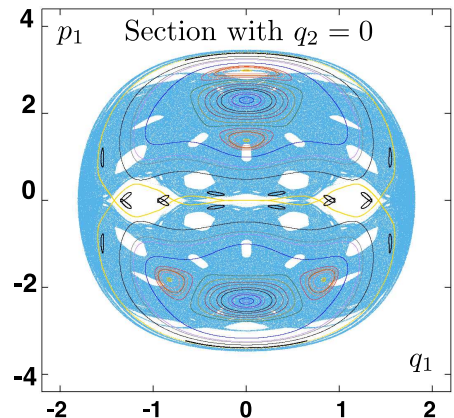


Fig. 5. Here we see penetrations of the  $(q_1, p_1)$  plane along trajectories of 50,000,000 timesteps each using 25 equally-spaced initial conditions,  $p_1^2 = 0, 0.5, 1.0, 1.5, \dots, 12$  and  $p_1^2 + p_2^2 = 12$ . This  $q_2 = 0$  projection shows traces of many tori as well as a black “chain of islands”. The last of these initial conditions produces the blue dots, which form the largest fat-fractal chaotic sea. Most of the remaining points are closed curves generated by stable tori. Note the 18 black curves mostly near  $p_1 = 0$  which correspond to a relatively complex torus which threads through the  $q_2 = 0$  hyperplane eighteen times. The corresponding initial momenta are  $p_1^2 = 11.5$ ;  $p_2^2 = 0.5$

It is important to see that for any choice of the pair of coordinates  $\{q_1, q_2\}$  Gibbs’ statistical mechanics establishes that the maximum-entropy distributions of the two momenta  $\{p_1, p_2\}$  are identical. Thus our finding  $\langle T_1 \rangle \neq \langle T_2 \rangle$  shows that the dynamics from Hamilton’s motion equations is not at all ergodic. For example, in the large chaotic sea the mean values of the kinetic temperatures of the two particles are

roughly (3.7<sub>4</sub>, 3.1<sub>7</sub>). We believe that an exact and simple deterministic time-reversible algorithm for the microcanonical ensemble can be based on an analog of Coriolis forces. The particle momenta,  $\{(p_x, p_y)\}$  or  $\{(p_x, p_y, p_z)\}$  can be *rotated* from time to time. Rotations do not change the kinetic energy or the relative probability at equilibrium. This demon-free improvement of Michael Creutz' algorithm [11] can be tailored to provide the microcanonical distribution for simple Hamiltonians like the cell model [12, 13]

#### IV. THE SNOOK PRIZE PROBLEM FOR 2018

The several previous  $\phi^4$  studies, carried out with a variety of system sizes and thermostatted boundary conditions [10], have established that the  $\phi^4$  model can be usefully described by Fourier's Law. These works also demonstrate that nonequilibrium phase-space distributions are fractal attractors, with dimensionalities which can lie far below the dimensionality of Gibbs' equilibrium distributions [9]. A systematic study could be made to show how the distribution of temperatures in a conducting chain approaches the Law as the number of degrees of freedom is increased beyond two. The two-body problem itself suggests a study of the phase-space boundaries separating the regions of chaos from regular tori and an analysis of the disappearance of the tori with increasing energy. The possibility of developing a time-reversible ergodic algorithm at constant energy has to be considered [13]. A study of clever ideas for the model would be welcome. The Snook Prize Problem is a detailed investigation of the two-body  $\phi^4$  problem from the standpoints of Hamiltonian chaos and Kolmogorov-Arnold-Moser tori and from the goal of an isoenergetic algorithm for the microcanonical Gibbs ensemble. It is particularly desirable that Prize entries be self-contained and pedagogical, stressing numerical findings in sufficient detail that their results can be corroborated.

#### Acknowledgments

We are grateful to the Institute of Bioorganic Chemistry of the Polish Academy of Sciences and to the Poznan Supercomputing and Networking Center for their joint support of these prizes honoring our late Australian colleague Ian Snook (1945-2013).

#### References

- [1] K. Aoki, D. Kusnezov, *Lyapunov Exponents and the Extensivity of Dimensional Loss for Systems in Thermal Gradients*, Physical Review E **68**, 056204 (2003).
- [2] K. Aoki, *Symmetry, Chaos, and Temperature in the One-Dimensional Lattice  $\phi^4$  Theory*, Computational Methods in Science and Technology **24** (2018) = arXiv 1801.02865. His arXiv version 1 contains the configurational part of our Figure 1. That figure is missing in version 2 and the internet version in CMST.
- [3] Wm.G. Hoover, C.G. Hoover, *The 2017 SNOOK PRIZES in Computational Statistical Mechanics*, Computational Methods in Science and Technology **24** (2018).
- [4] T. Hofmann, J. Merker, *On Local Lyapunov Exponents of Chaotic Hamiltonian Systems*, Computational Methods in Science and Technology **24** (2018).
- [5] G. Benettin, L. Galgani, A. Giorgilli, J.-M. Strelcyn, *Lyapunov Characteristic Exponents for Smooth Dynamics Systems and for Hamiltonian Systems; a Method for Computing All of Them, Parts I and II: Theory and Numerical Application*, Meccanica **15**, 9–20 and 21–30 (1980).
- [6] I. Shimada, T. Nagashima, *A Numerical Approach to Ergodic Problems of Dissipative Dynamical Systems*, Progress of Theoretical Physics **61**, 1605–1616 (1979).
- [7] J.D. Farmer, E. Ott, J.A. Yorke, *The Dimension of Chaotic Attractors*, Physica D **7**, 153–180 (1983).
- [8] Wm.G. Hoover, C.G. Hoover, *Nonequilibrium Temperature and Thermometry in Heat-Conducting  $\phi^4$  Models*, Physical Review E **77**, 041104 (2008).
- [9] Wm.G. Hoover, C.G. Hoover, *Microscopic and Macroscopic Simulation Techniques – Kharagpur Lectures*, Section 10.8 (World Scientific Publishers, Singapore, 2018).
- [10] Wm.G. Hoover, K. Aoki, C.G. Hoover, S.V. De Groot, *Time-Reversible Deterministic Thermostats*, Physica D **187**, 253–267 (2004).
- [11] M. Creutz, *Microcanonical Monte Carlo Simulation*, Physical Review Letters **50**, 1411–1414 (1983).
- [12] Wm.G. Hoover, C.G. Hoover, *Comparison of Very Smooth Cell-Model Trajectories Using Five Symplectic and Two Runge-Kutta Integrators*, Computational Methods in Science and Technology **21** 109–116 (2015). Note that the second-order Leapfrog algorithm at the top of page 111 is missing a factor of  $dt^2$  just after the “ $\equiv$ ” sign.
- [13] Wm.G. Hoover, C.G. Hoover, *Ergodic Isoenergetic Molecular Dynamics for Microcanonical-Ensemble Averages* (arXiv 1806.09802, 2018).



**William G. Hoover, Carol G. Hoover;** Bill and Carol Hoover live in Ruby Valley (Elko County Nevada) where the cows outnumber the people by orders of magnitude and the phonebook is a single page. Their research interests include chaos, fractals, symmetry breaking instabilities, and computer simulations linking the microscopic and macroscopic descriptions of nonequilibrium processes. Their most recent book is Reference [9].